Microchimica Acta
https://doi.org/10.1007/s00604-018-2722-9

ORIGINAL PAPER

Enzymatic biosensing by covalent conjugation of enzymes to 3D-networks of graphene nanosheets on arrays of vertically aligned gold nanorods: Application to voltammetric glucose sensing

Mozhdeh Mazaheri[1] · Abdolreza Simchi[1,2] · Hossein Aashuri[1]

Received: 29 November 2017 / Accepted: 31 January 2018

Abstract
The authors demonstrate efficient direct electron transfer from the enzyme glucose oxidase to vertically aligned gold nanorods with a diameter of ~160 nm and a length of ~2 μm that are covalently linkage to a 3-dimensional network of reduced graphene oxide nanosheets. The assembly can be prepared by a 2-step electrochemical procedure. This hybrid structure holds the enzyme in a favorable position while retaining its functionality that ultimately provides enhanced performance for enzymatic sensing of glucose without utilizing mediators. The nanorod assembly was applied to the voltammetric detection of glucose. Figures of merit include an electrochemical sensitivity of 12 $\mu A \cdot mM^{-1} \cdot cm^{-2}$ (obtained from cathodic peak current at a voltage of −0.45 V vs. Ag/AgCl), a 3 μM detection limit (at signal/noise = 3), and a wide linear range (0.01–7 mM). The hybrid nanostructure has a heterogeneous electron transfer rate constant (k_s) of 2.9 s^{-1}. The high electrochemical activity is attributed to the synergistic effect of a large active surface and an enhanced electron transfer efficiency due to covalent amide linkage.

Keywords Biosensor · Carbon nanostructures · Reduced graphene oxide · Nanosheets · Glucose oxidase · Electrochemistry · Differential Pulse Voltammetry (DPV)

Introduction

Electrochemical biosensors based on the direct electrochemistry of enzymes without the assistance of mediators have gained considerable attention due to their outstanding features such as high selectivity, good sensitivity and comparative low cost [1, 2]. Many efforts have been carried out to develop nanomaterials including metals [3], metallic oxides [4] and carbon nanostructures [5] as matrices for enzyme immobilization to achieve direct electron transfer of redox enzymes. In this context, gold nanostructures with excellent catalytic and electron transfer properties have been extensively used in biosensors due to their biocompatibility and high effective surface area [6, 7]. Gold nanomaterial such as nanorods (NRs) can improve the sensitivity of the electrochemical sensors. However, to achieve the high surface of these nanomaterials, orientation of the AuNRs is an important factor. Vertically aligned NRs have shown more functionality than nanorods with random configuration [8, 9]. On the other hand, carbon nanomaterials with unique features such as a high surface-to-volume ratio, high electrical conductivity, chemical stability and robust mechanical strength are frequently incorporated as sensing elements [10]. Graphene, a single layer of carbon atoms with 2D honeycombed lattice, has a unique ability to promote fast electron transfer kinetics for a wide range of electroactive species [11, 12]. The absorption or covalent attachment of enzymes to functional groups of graphene enables direct electron transfer from the redox groups of enzymes such as glucose oxidase (GOx) to the electrode surface. Combining these materials with noble metal nanostructures simplifies enzyme immobilization

Electronic supplementary material The online version of this article (https://doi.org/10.1007/s00604-018-2722-9) contains supplementary material, which is available to authorized users.

✉ Abdolreza Simchi
simchi@sharif.edu

[1] Department of Materials Science and Engineering, Sharif University of Technology, Azadi Avenue, P.O. Box 11365-9466, Tehran, Iran

[2] Institute for Nanoscience and Nanotechnology, Sharif University of Technology, Azadi Avenue, P.O. Box 11365-9466, Tehran, Iran

Published online: 14 February 2018

and enhances the surface area [13]. Many studies have shown that hybrid graphene/gold biosensors offer a favorable microenvironment for facilitating direct electron transfer between enzyme and the electrode [14]. Improved performance and stability for cholesterol detection by gold nanoparticles (NPs) decorated graphene nanoplatelets [11] and enzymatic glucose detection by graphene/polyaniline/gold nanoparticles nanocomposite modified glassy carbon electrode [1] have also been demonstrated.

The authors show that covalent amid conjugation of an enzyme model to reduced graphene oxide (rGO) nanosheets enhances the direct charge transfer to gold nanostructures. This finding is of particular importance for the fabrication of next generation enzymatic biosensors based on carbon-metal hybrid nanocomposites. A two-step electrochemical procedure was employed to prepare the conjugated enzyme/graphene nanosheets/gold nanorods assembly. The procedure is schematically shown in Fig. 1. Vertically aligned arrays of gold were prepared by template-assisted electrochemical growth. Then, the enzyme-graphene oxide nanosheets were assembled into three-dimensional networks and electrochemically immobilized onto the gold arrays where the graphene oxide sheets were reduced simultaneously. It is shown that the high-surface area of the hybrid structure and the direct electron transfer from the immobilized enzyme to the gold nanostructure facilitated by the graphene network provide a favorite platform for electrochemical enzymatic detection of biomolecules.

Experimental

Materials

HNO_3 (65%), H_2SO_4 (95–98%), H_2O_2 (30%), HCl (37%), $KMnO_4$, $NaNO_3$, uric acid (UA) and ascorbic acid (AA) were obtained from Merck (Darmstadt, Germany, http://www.merckmillipore.com), D-(+)-glucose (>98%) and dichloromethane (99.8%) were purchased from Samchun chemical Co. (Seoul, Korea, http://www.samchun.com). Glucose oxidase (GOx, EC 1.1.3.4) from Aspergillus Niger (Type X-S) was obtained from Sigma-Aldrich (St. Louis, MO, USA, https://www.sigmaaldrich.com). Nucleopore track-etched polycarbonate (PC) membrane (diameter = 25 mm) with a pore size of 100 nm and a thickness of 6 μm was purchased from Whatman Ltd., UK. Graphite powder and other reagents employed were of analytical grade and used as received without any purification. All aqueous solutions were prepared in deionized (DI) water (>18 MΩ·cm).

Instruments

Topographic image of the GO sheets was gained using an atomic force microscope (AFM, CP-Research, Veeco Instruments Inc., USA) in non-contact mode. UV-visible spectrum of GO suspension was recorded on a spectrometer (Lambda 35, Perkin-Elmer, USA) from 200 to 900 nm. X-ray diffraction (XRD) patterns were collected with an X-ray diffractometer (Philips, X'pert PRO, The Netherlands) using Cu Kα radiation (λ = 1.54 Å). Scanning electron micrographs were taken out on a field emission scanning electron microscope (MIRA 3, TESCAN, Czech Republic) with energy dispersive X-ray spectroscopy (EDS) equipment at an accelerating voltage of 15 kV. X-ray photoelectron spectra were recorded on an X-ray photoelectron spectrometer (8025-BesTec, Germany) equipped with an Al Kα X-ray source (h_v = 1486.6 eV) in ultra-high vacuum. All electrochemical studies were performed at room temperature using an Autolab PGSTAT302N electrochemical workstation (Eco-Chemie, The Netherlands) with a conventional three-electrode configuration consisting of the modified electrodes as working electrodes, a platinum (Pt) wire as auxiliary electrode, and Ag/AgCl (in saturated KCl) as the reference electrode. The details of analytical procedures are explained in Electronic Supplementary Material (ESM).

Preparation of graphene oxide nanosheets

Graphene oxide nanosheets were prepared from the graphite powder using modified Hummer's method as described elsewhere [15, 16]. Chemical oxidation of graphite powder was performed by a $NaNO_3/KMnO_4/H_2SO_4$ mixture, as explained in ESM. The product was ultrasonically exfoliated to obtain individual graphene oxide sheets. According to AFM analysis presented in ESM (Fig. S1a), the thickness of graphene oxide sheets was about 1 nm, revealing that complete exfoliation of graphite oxide was achieved. The successful synthesis of the GO was also confirmed by UV-Vis, XPS and Raman spectroscopy (Fig. S1b to S1d).

Fabrication of Au nanorods array

For the electrodeposition of gold nanorods (AuNRs), at first a thin film of gold (~30 nm) was sputtered onto one side of the PC template to make it conductive. Before Au electrodeposition, the PC membrane was ultrasonicated in DI water for 5 min in order to wet inside the pores. The electrodeposition of AuNRs was performed at ambient temperature in a two-electrode cell, as shown in Fig. S2. The Au-backed template was placed on a copper sheet to serve as the working electrode and a Pt plate was used as a counter-electrode. The distance between the two electrodes was kept at 10 mm. The working solution was 5 mL gold (III) solution (0.1 wt.%) which was

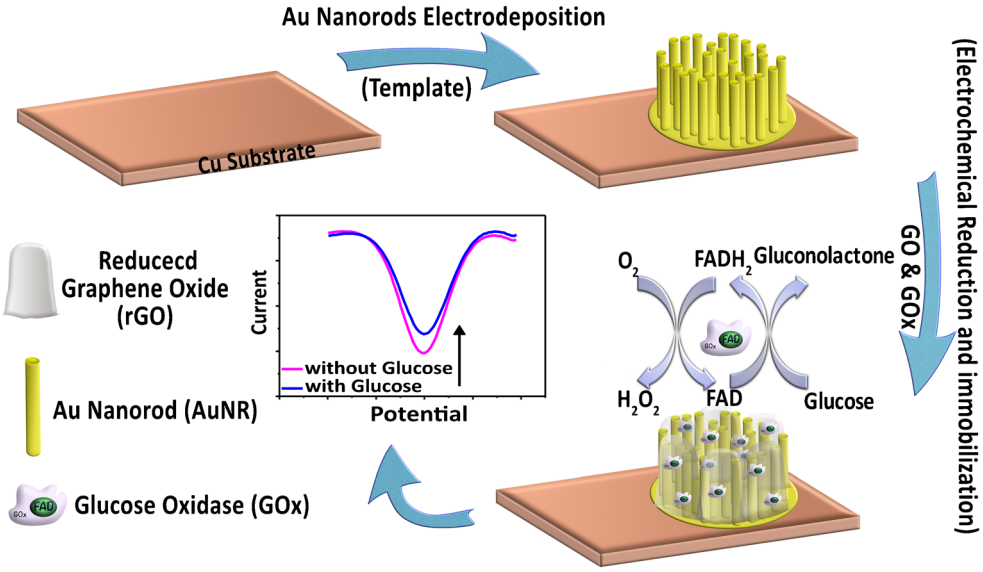

Fig. 1 Schematic of procedures used for the preparation of enzyme-functionalized graphene networks immobilized onto vertically aligned gold nanorods array

prepared by dissolving 1 g gold foil (99.99%) into aqua regia solution as described in ESM. AuNRs were deposited into the pores of PC membrane by applying a constant potential of −4.0 V on Cu sheet for 40 min. Next, a thin layer of nickel was electrodeposited onto back-side of the AuNRs using a mixture of 70 $g{\cdot}L^{-1}$ $NiSO_4 \cdot 7H_2O$, 20 $g{\cdot}L^{-1}$ $NiCl_2{\cdot}6H_2O$ and 15 $g{\cdot}L^{-1}$ H_3BO_3. The electrodeposition was performed at a potential of −3.0 V for 10 min to increase the strength of the electrode. After Ni electrodeposition, the PC template was attached nickel-side down on a conductive copper tape and the template was dissolved by immersing in dichloromethane for 30 min. Then, it was washed with deionized water and dried in air.

Fabrication of hybrid enzyme/reduced graphene oxide/gold nanorod electrodes

For enzyme immobilization, 5.0 mg GOx powder was dissolved in 1.0 mL of 0.1 M phosphate buffer (PB, pH 5.0). The solution was then mixed with GO suspension (1.0 $mg{\cdot}mL^{-1}$) at a 1:1 ratio (v/v). Then, 10 μL of GOx/GO mixture was drop casted onto AuNRs electrode and the electrode dried at room temperature. The prepared electrode, which is denoted as GOx/GO/AuNR, was gently washed with deionized water to remove loosely adsorbed enzyme molecules. Finally, GOx/rGO/AuNR electrode was obtained using five consecutive cyclic voltammetry (CV) of GOx/GO/AuNR in 0.01 M nitrogen saturated phosphate buffer (pH 7.0). The successive CVs were carried out in potential range from 0 to −1.3 V at a scan rate of 50 $mV{\cdot}s^{-1}$ [17]. Moreover, AuNRs, rGO/AuNR and GOx/AuNR were prepared for comparison. In order to explore the role of gold morphology, enzyme-graphene oxide assembly was immobilized on planar gold substrates that is denoted as GOx/rGO/Au (planar). The enzyme-modified electrodes were stored in 4 °C when not in use.

Results and discussion

Choice of materials

The choice of materials is the most important step in the design of a biosensing system. In this context, gold nanorods, especially with vertical orientation have gained considerable attention for electrochemical biosensing with some advantages over gold nanoparticles including high surface area and fast electron transport characteristics [18]. On the other hand, graphene oxide and its derivatives with 2-dimensional structure and oxygen functional groups provide a suitable matrix for biomolecules immobilization. Moreover, GO is produced from cheap graphite without metallic impurities that makes it a better choice for many applications as compared with carbon nanotubes (CNT) [19]. So, utilizing rGO/gold nanorods array as the electrode material for GOx immobilization can be a promising platform for sensitive detection of glucose.

Electrochemical reduction of GO nanosheets and electrode stabilization

During successive CVs, the electrochemical reduction of graphene oxide nanolayers is susceptible. Fig. S3 shows the cyclic voltammogram (5 cycles) of the enzyme-graphene oxide immobilized AuNR during the reduction process at a scan rate of 50 $mV{\cdot}s^{-1}$. At the first cycle, an intense reduction peak is seen at ~ −0.9 V, which is ascribed to the reduction of various functional groups on GO sheets [5]. This peak is not

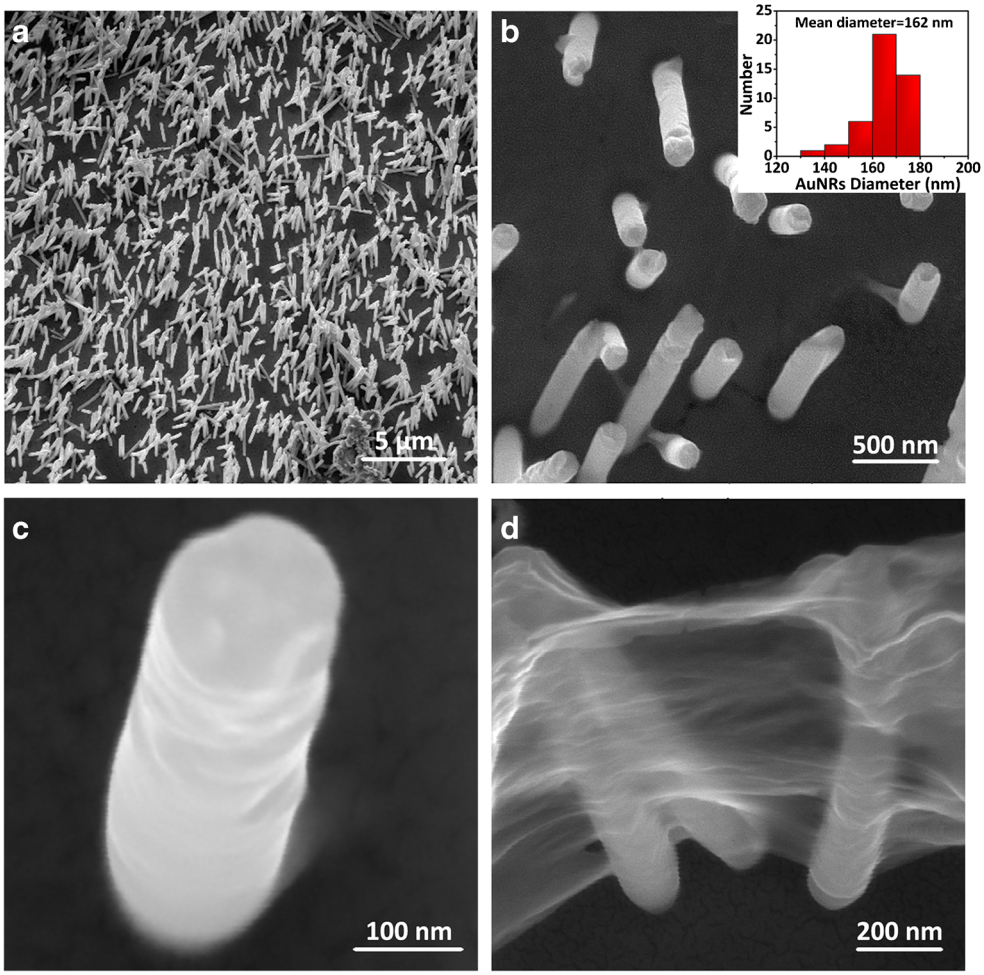

Fig. 2 Characterizations of the prepared nanostructures. (a) to (c) SEM images show the structure of the gold nanorod array (d) SEM images determine folded and wrinkled graphene nanosheets embedded in the gold nanorods arrays

detected after further potential cycling; however, a pair of redox peaks emerges in the potentials around −0.5 V that corresponds to redox couple of GOx(FAD)/GOx($FADH_2$). This experiment confirmed conjugation of the enzyme-rGO nanosheets on AuNRs. This procedure was employed to reduce the surface functional groups of GO nanosheets (forming rGO) and to stabilize the electrodes for further studies.

Characterizations of the electrodes

The structure of the functionalized hybrid nanostructure is shown in Fig. 2. Electrochemical deposition of gold inside PC template resulted in the formation of gold nanorods with diameters of about 160 nm. The density of gold nanorods is ca. 3×10^6 number·mm^{-2} with a length of ~2 μm (Figs. 2a to 2c). Coating of graphene nanosheets formed a three-dimensional network of graphene embedded into the gold nanorods structure (Figs. 2d). EDS (Fig. S4a) confirmed the presence of gold, carbon and oxygen. The thin folded and wrinkled morphology of graphene enhances the electrode active surface area of the hybrid system to attain improved electrocatalytic performance.

FTIR measurements indicated change in the absorption band after conjugation and electrochemical process (Fig. S4b). The synthesized graphene oxide had different oxygen functional groups including stretching vibrations of C-O in alkoxy (at 1052 cm^{-1}) and epoxy (at 1236 cm^{-1}), C=O stretching of the carboxylic group (at 1675 cm^{-1}), in plane vibrations of sp^2-hybridized C=C (at 1605 cm^{-1}), and OH and the absorbed water molecule (at 3400 cm^{-1}) [20, 21]. The IR spectrum of the model enzyme (glucose oxidase) showed the N − H stretching vibrations at 3305 cm^{-1}, the amide I at 1656 cm^{-1} (the C=O stretching vibrations of the peptide bond groups), amide II at 1538 cm^{-1} (the N − H in-plane bending and C − N stretching modes of the polypeptide chains), and C-O stretching vibrations at 1102 cm^{-1} bands [22, 23]. After consecutive cyclic voltammetry of the enzyme-graphene oxide, the successful reduction of GO was confirmed by the decrease in the intensity or disappearance of various functional groups peaks (Fig. S4b). On the other hand, in the immobilized enzyme, the amide I and II bands were shifted slightly. These changes in the absorption bands suggested a covalent linkage of free amino group of enzyme to the carboxylic group of rGO nanosheets [24].

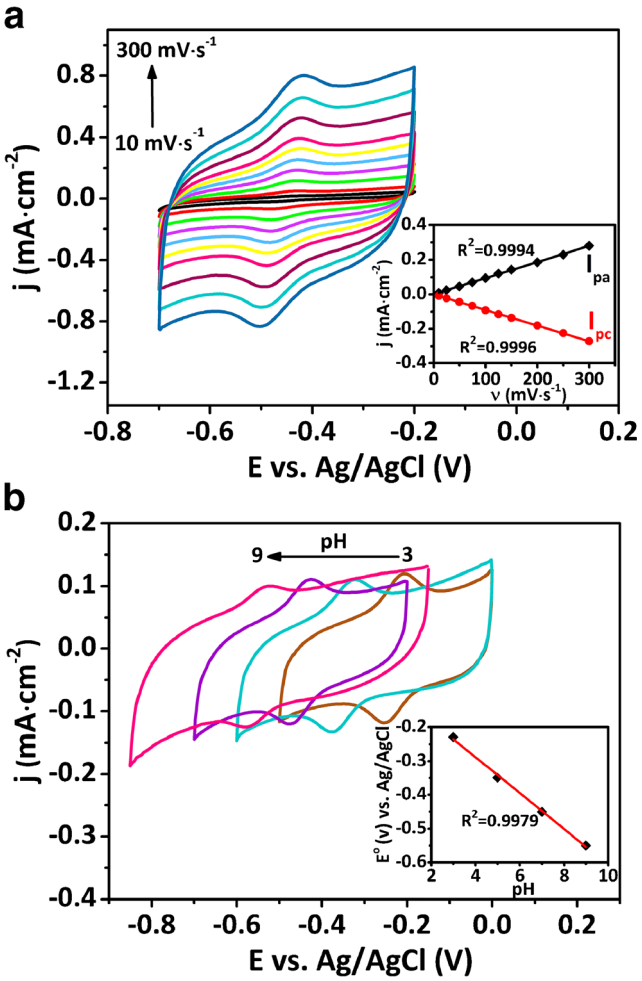

Fig. 3 (a) Effect of scan rate (from 10 to 300 mV·s^{-1}; from inner to outer) on CV of the enzyme-functionalized graphene/gold arrays in N_2-saturated phosphate buffer (pH 7.0). Inset shows variations of cathodic and anodic peak currents as a function of scan rate. (b) Effect of buffer pH (from 3 to 9) on CV of enzyme-functionalized graphene/gold arrays in oxygen-free phosphate buffer at a scan rate of 50 mV·s^{-1}. The inset shows the formal potential versus pH

Fig. S4c shows XRD pattern of the hybrid nanocomposite. The characteristic peaks of gold (JCPDS cards Au: No.04–0784) were detected. The other diffraction peaks were related to the substrate while the characteristic peaks of graphene were not visible due to its low volume fraction. However, the XRD pattern of pristine graphene oxide exhibited the diffraction peak at about 11.3° corresponding to the (001) crystalline plane with an interlayer spacing of ~ 0.78 nm.

Electrochemical properties of the enzyme electrode

The direct electrochemistry of immobilized GOx on different electrodes was assessed by cyclic voltammetry in N_2-saturated phosphate buffer (Fig. S5a). In general, the 3D GOx/rGO/AuNR electrode demonstrated the best performance with enhanced redox peak current (See ESM for more details). The results indicated the important role of Au morphology and the graphene network on enzyme immobilization. The hybrid nanostructure facilitated the direct electron transfer from the active site of GOx to the electrode. It seems that the higher effective surface area of gold nanorods provides more sites for enzyme immobilization. Moreover, as shown in Fig. S5b CVs of the GOx/rGO/AuNR electrode remained almost unchanged even after 20 consecutive scans in N_2-saturated buffer (pH 7.0), demonstrating the good stability of the immobilized GOx on the electrode surface.

To further investigate the direct electron transfer between the enzyme and gold nanorods supported by rGO, the effect of scan rate and buffer pH were studied under nitrogen atmosphere. Fig. 3a shows that both anodic and cathodic peak currents increased with the scan rate in a linear way with marginal changes in the corresponding potentials and I_{pa}/I_{pc} ratio (approximately equal to unity). Therefore, it was suggested that a quasi-reversible surface-controlled redox reaction controlled the electron transfer process, as expected for immobilized systems [25]. On the other hand, there is a linear relationship between the peak potential and the logarithm of scan rate at high scan rates (Fig. S6). According to Laviron's model [26] for $n\Delta E_p > 200$ mV:

$$E_{pa} = E^{'0} + [RT/(1-\alpha)nF]\ln[(1-\alpha)/m] \quad (1)$$

$$E_{pc} = E^{'0} - (RT/\alpha nF)\ln[\alpha/m] \quad (2)$$

$$\log k_s = \alpha\log(1-\alpha) + (1-\alpha)\log\alpha - \log(RT/nF\nu) - \alpha(1-\alpha)nF\Delta E_p/2.3\,RT \quad (3)$$

where m is (RT/F) $(k_s/n\nu)$, α is charge transfer coefficient, k_s is the rate constant of the electrochemical reaction (s^{-1}), F is Faraday constant, n is the number of electron transferred in the rate-determining step, and other parameters have their usual meanings. From the slope of two straight lines in Fig. S6, α was calculated as 0.43. Based on Eq. 3, the value of k_s was determined to be 2.9 s^{-1}, which is higher than those reported for GOx@flower-shaped graphene microelectrode (2.18 s^{-1}) [27], Nafion/GOx/AuNP@MoS_2 (1.10 s^{-1}) [2] and Nafion/GOx/rGO (0.96 s^{-1}) [28].

As the redox reaction of FAD/$FADH_2$ couple in the enzyme is a proton-coupled electron transfer reaction [5], pH of the working solution affects the electron transfer process. As shown in Fig. 3b, both anodic and cathodic peak potentials of the FAD/$FADH_2$ redox couple in the GOx modified electrode were negatively shifted with the pH change from 3 to 9. The formal potential showed a linear relation with buffer pH with the slope of −53.2 mV·pH^{-1} ($R^2 = 0.9979$). This value is close to the theoretical value (about −59 mV·pH^{-1} at 25 °C) obtained from the Nernst equation for reduction reaction of GOx(FAD), indicating that two electrons and two protons are involved in the electron transfer process. In order to simulate

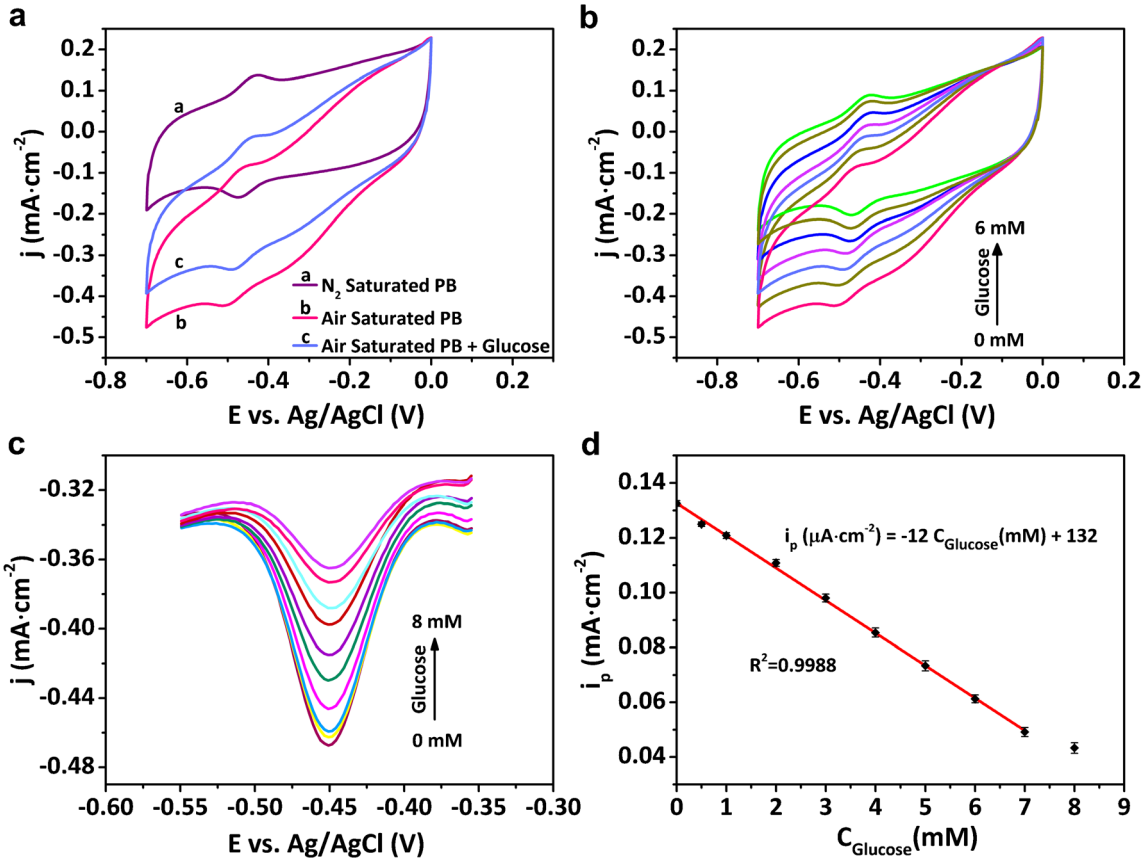

Fig. 4 Effects of oxygen and glucose concentration on the redox reaction of the 3D hybrid electrode. (a) CV responses in N_2-saturated PB and in the air-saturated PB before and after addition of glucose (final concentration of 2.0 mM). (b) CV responses in various concentrations of glucose in 0.01 M PB solution (from 0 to 6 mM) at a scan rate of 50 mV·s^{-1}. (c) DPV curves in 0.01 M PB (pH 7.0) containing different concentration of glucose at a scan rate of 10 mV·s^{-1}. (d) Dependence of the peak current measured at potential of −0.45 V (vs. reference electrode) on the glucose concentration

the physiological environment, phosphate buffer with pH value of 7.0 was used for further investigation.

Electrocatalytic behavior of the hybrid electrode

The role of dissolved oxygen in the electrolyte (0.01 M PB at pH 7.0) on the redox reactions was studied. Fig. 4a indicates significant difference in CV responses of the 3D hybrid nanocomposite in air-saturated and nitrogen-saturated solutions. In the deoxygenated solution, near symmetrical redox peak of FAD/$FADH_2$ couple in the GOx was visible. However, in the presence of dissolved oxygen, the reduction peak current of GOx(FAD) was enhanced dramatically, while the oxidation peak current was reduced. This indicated that GOx($FADH_2$), which was generated

Table 1 Figure of merits for the hybrid electrode as compared with other enzymatic glucose biosensors

Electrode	Method	Linear range (mM)	Detection limit (μM)	Sensitivity (μA·mM^{-1}·cm^{-2})	Ref.
rGO-GOx/GCE[(a)]	Amperometry	0.1–27	–	1.85	[17]
Graphene/CNT[(b)]/ZnO/GOx	DPV	0.01–6.5	4.5	5.36	[31]
HNT[(c)]/AgNP/GOx	CV	0.2–6	–	5.2	[32]
GOx/Graphene/PANI[(d)]/AuNP/GCE	Amperometry	0.004–1.12	0.6	–	[1]
GOx/Au nanoprism/Chitosan/GCE	CV	0.05–1.2	10	11.83	[29]
Graphene/MWCNTs[(e)]/AuNP/GOx	Amperometry	0.01–2.0 2.0–5.2	4.1 950	0.695 0.238	[30]
GOx/Graphene/AuNP/GCE	Amperometry	0.02–2.26	4.1	3.844	[33]
GOx/rGO/AuNR	DPV	0.01–7.0	3	12	This work

(a) Glassy Carbon Electrode; (b) Carbon Nanotube; (c) Halloysite nanotubes; (d) Polyaniline; (e) Multiwalled Carbon Nanotubes

Table 2 Determination of glucose in human serum samples ($n = 3$)

Serum Sample	Measured Concentration (mM)			Relative Error (%)
	Commercial glucometer	The hybrid electrode	RSD (%)	
1	5.85 ± 0.11	5.71 ± 0.25	4.43	2.39
2	5.57 ± 0.09	5.35 ± 0.11	2.08	3.94
3	4.53 ± 0.06	4.37 ± 0.12	2.70	3.53

by reduction of GOx(FAD) in the cathodic half cycle, catalyzed the oxygen reduction reaction according to following equation:

$$GOx\ (FADH_2) + O_2 \rightarrow GOx\ (FAD) + H_2O_2 \quad (4)$$

Thus, the dissolved oxygen increased the reduction peak current. A new reduction peak was also appeared at about −0.35 V in the air-saturated phosphate buffer that is due to the oxygen reduction on the electrode surface. After the addition of glucose to 0.01 M air-saturated PB (pH 7.0), the cathodic peak current decreased due to consumption of dissolved O_2 during the enzyme-catalyzed reaction between the GOx(FAD) and glucose (Eq. 5).

$$GOx\ (FAD) + Glucose \rightarrow GOx\ (FADH_2) + Gluconolactone \quad (5)$$

The sensing response of the 3D hybrid nanocomposite was studied by CV measurements in air-saturated buffer (pH 7.0) (Fig. 4b). As seen, with increasing the biomolecule concentration, the reduction current gradually decreased. The response of the electrode based on a decrease in the reduction current is useful for the development of a sensitive biosensor.

Differential pulse voltammetry (DPV) was employed to obtain the calibration plot. DPV responses of the hybrid electrode at different concentrations of the glucose in buffer (pH 7.0) are shown in Fig. 4c. The curves displayed well-defined reduction peak at a potential of ~ −0.45 V, while the cathodic peak current was reduced with the successive addition of the biomolecules. Fig. 4d shows a linear relationship ($R^2 = 0.9988$) between the cathodic peak current and the concentration in the range of 0.01 to 7 mM. The sensitivity of 12 $\mu A \cdot mM^{-1} \cdot cm^{-2}$ was calculated from the slope of the calibration plot. The limit of detection of 3 μM (Signal/Noise = 3) was obtained which is lower than that of electrodes such as GOx/Au nanoprism/chitosan and graphene-multiwalled carbon nanotubes/AuNP/GOx biosensors [29, 30]. Table 1 compares the analytical features of the prepared electrode with some enzyme-based glucose biosensors. The satisfying performance of the modified electrode can be ascribed to the combination of excellent electrocatalytic properties with large surface area provided by the 3D hybrid structure.

Selectivity, repeatability and real sample analysis

The specificity of the GOx/rGO/AuNR biosensor for glucose was evaluated using the DPV method. The voltammetric response of the hybrid electrode in 0.01 M PB containing 2 mM glucose in the absence and presence of 0.5 mM AA or 0.5 mM UA is shown in Fig. S7. No obvious change in the catalytic current was noticed in the presence of these electroactive species. The results determined good selectivity of the 3D biosensor that can be due to the low working potential. Also, repeatability of the hybrid biosensor was investigated by four successive voltammetry measurements in buffer containing 5 mM glucose. The relative standard deviation (RSD) was only 1.8%, suggesting a good repeatability.

Finally, the practical applications of the hybrid electrode for glucose detection in human blood serum was studied and the glucose concentration in real samples was measured by the electrode. As can be seen in Table 2, the results determined from the hybrid biosensor were in good agreement with those obtained by the commercial glucometer. These results suggest that the 3D hybrid electrode has a great potential for enzymatic biosensing applications.

Conclusions

In summary, enzyme-functionalized graphene networks immobilized on vertically aligned gold nanorods were fabricated. Enhanced electron transfer from the enzyme to the gold nanostructure by covalent conjugation with 3D networks of rGO nanosheets was shown. It was demonstrated that a quasi-reversible surface-controlled redox reaction controlled the electron transfer process. The redox reaction of the enzyme on the electrode surface was demonstrated to vary with pH, scan rate, and oxygen concentration in the buffer. To show the potential application of the hybrid biosensor, *in vitro* glucose detection in phosphate buffer and human blood serum was examined. A wide linear range, low-level detection limit, good selectivity and high sensitivity were revealed the high electrochemical activity of the hybrid electrode. Nonetheless, the sensitivity was lower than that of enzyme-free sensors. Moreover, it should be mentioned that the control of enzyme orientation on the electrode remained a main challenge that affected the reproducibility of the biosensor.

Acknowledgements This work was supported by the Grant Program of Sharif University of Technology (No. G930305) and Iran National Science Foundation (INSF No. 95-S-48740).

Compliance of ethical standards

All utilized procedures were in accordance with relevant guidelines and regulations of the Sharif University of Technology. The work has been approved by the ethical committee and all the patients signed an informed consent form.

Conflicts of interest There are no conflicts to declare.

References

1. Xu Q, Gu S-X, Jin L, Y-e Z, Yang Z, Wang W, Hu X (2014) Graphene/polyaniline/gold nanoparticles nanocomposite for the direct electron transfer of glucose oxidase and glucose biosensing. Sens Actuators B: Chem 190:562–569. https://doi.org/10.1016/j.snb.2013.09.049
2. Liang B, Fang L, Yang G, Hu Y, Guo X, Ye X (2013) Direct electron transfer glucose biosensor based on glucose oxidase self-assembled on electrochemically reduced carboxyl graphene. Biosens Bioelectron 43:131–136. https://doi.org/10.1016/j.bios.2012.11.040
3. Hasan A, Nurunnabi M, Morshed M, Paul A, Polini A, Kuila T, Al Hariri M, Lee Y-K, Jaffa AA (2014) Recent Advances in Application of Biosensors in Tissue Engineering. Biomed res int 2014 (Article ID 307519):1–18 doi:https://doi.org/10.1155/2014/307519
4. Zhao Y, Li W, Pan L, Zhai D, Wang Y, Li L, Cheng W, Yin W, Wang X, Xu J-B (2016) ZnO-nanorods/graphene heterostructure: a direct electron transfer glucose biosensor. Sci Rep 6:32327. https://doi.org/10.1038/srep32327
5. Mani V, Devadas B, Chen S-M (2013) Direct electrochemistry of glucose oxidase at electrochemically reduced graphene oxide-multiwalled carbon nanotubes hybrid material modified electrode for glucose biosensor. Biosens Bioelectron 41:309–315. https://doi.org/10.1016/j.bios.2012.08.045
6. Ramulu T, Venu R, Sinha B, Lim B, Jeon S, Yoon S, Kim C (2013) Nanowires array modified electrode for enhanced electrochemical detection of nucleic acid. Biosens Bioelectron 40(1):258–264. https://doi.org/10.1016/j.bios.2012.07.034
7. Pandey P, Singh S, Arya SK, Sharma A, Datta M, Malhotra BD (2008) Gold nanoparticle-polyaniline composite films for glucose sensing. J Nanosci Nanotechnol 8(6):3158–3163. https://doi.org/10.1166/jnn.2008.349
8. García-Carmona L, González MC, Escarpa A (2017) Vertically-Oriented and Shape-Tailored Electrocatalytic Metal Nanowire Arrays for Enzyme-Free Galactosemia Rapid Diagnosis. Chem Eur J 23(38):9048–9053. https://doi.org/10.1002/chem.201701213
9. García-Carmona L, Moreno-Guzmán M, Martín A, Martínez SB, Fernández-Martínez AB, González MC, Lucio-Cazaña J, Escarpa A (2017) Aligned copper nanowires as a cut-and-paste exclusive electrochemical transducer for free-enzyme highly selective quantification of intracellular hydrogen peroxide in cisplatin-treated cells. Biosens Bioelectron 96:146–151. https://doi.org/10.1016/j.bios.2017.04.048
10. Chen A, Chatterjee S (2013) Nanomaterials based electrochemical sensors for biomedical applications. Chem Soc Rev 42(12):5425–5438. https://doi.org/10.1039/C3CS35518G
11. Aravind SSJ, Baby TT, Arockiadoss T, Rakhi RB, Ramaprabhu S (2011) A cholesterol biosensor based on gold nanoparticles decorated functionalized graphene nanoplatelets. Thin Solid Films 519(16):5667–5672. https://doi.org/10.1016/j.tsf.2011.03.032
12. Vijayaraj K, Hong SW, Jin S-H, Chang S-C, Park D-S (2016) Fabrication of a novel disposable glucose biosensor using an electrochemically reduced graphene oxide–glucose oxidase biocomposite. Anal Methods 8(38):6974–6981. https://doi.org/10.1039/C6AY02032A
13. Luong JH, Glennon JD, Gedanken A, Vashist SK (2017) Achievement and assessment of direct electron transfer of glucose oxidase in electrochemical biosensing using carbon nanotubes, graphene, and their nanocomposites. Microchim Acta 184(2):369–388. https://doi.org/10.1007/s00604-016-2049-3
14. Wang L, Yu J, Zhang Y, Yang H, Miao L, Song Y (2017) Simple and Large-Scale Strategy to Prepare Flexible Graphene Tape Electrode. ACS Appl Mater Interfaces 9(10):9089–9095. https://doi.org/10.1021/acsami.6b14624
15. Hummers WS Jr, Offeman RE (1958) Preparation of graphitic oxide. J Am Chem Soc 80(6):1339–1339. https://doi.org/10.1021/ja01539a017
16. Mazaheri M, Aashuri H, Simchi A (2017) Three-dimensional hybrid graphene/nickel electrodes on zinc oxide nanorod arrays as non-enzymatic glucose biosensors. Sens Actuators B: Chem 251:462–471. https://doi.org/10.1016/j.snb.2017.05.062
17. Unnikrishnan B, Palanisamy S, Chen S-M (2013) A simple electrochemical approach to fabricate a glucose biosensor based on graphene–glucose oxidase biocomposite. Biosens Bioelectron 39(1):70–75. https://doi.org/10.1016/j.bios.2012.06.045
18. Qian D, Li W, Chen F, Huang Y, Bao N, Gu H, Yu C (2017) Voltammetric sensor for trichloroacetic acid using a glassy carbon electrode modified with Au@ Ag nanorods and hemoglobin. Microchim Acta 184(7):1977–1985. https://doi.org/10.1007/s00604-017-2175-6
19. Pumera M, Ambrosi A, Bonanni A, Chng ELK, Poh HL (2010) Graphene for electrochemical sensing and biosensing. TrAC Trends Anal Chem 29(9):954–965. https://doi.org/10.1016/j.trac.2010.05.011
20. Zhang Y, Pan C (2011) TiO_2/graphene composite from thermal reaction of graphene oxide and its photocatalytic activity in visible light. J Mater Sci 46(8):2622–2626. https://doi.org/10.1007/s10853-010-5116-x
21. Aunkor M, Mahbubul I, Saidur R, Metselaar H (2016) The green reduction of graphene oxide. RSC Adv 6(33):27807–27828. https://doi.org/10.1039/C6RA03189G
22. Zhang J, Yu X, Guo W, Qiu J, Mou X, Li A, Liu H (2016) Construction of titanium dioxide nanorod/graphite microfiber hybrid electrodes for a high performance electrochemical glucose biosensor. Nano 8(17):9382–9389. https://doi.org/10.1039/C6NR01360K
23. de Jesus CG, Lima D, dos Santos V, Wohnrath K, Pessôa CA (2013) Glucose biosensor based on the highly efficient immobilization of glucose oxidase on layer-by-layer films of silsesquioxane polyelectrolyte. Sens Actuators B: Chem 186:44–51. https://doi.org/10.1016/j.snb.2013.05.063
24. Sehat AA, Khodadadi AA, Shemirani F, Mortazavi Y (2015) Fast immobilization of glucose oxidase on graphene oxide for highly sensitive glucose biosensor fabrication. Int J Electrochem Sci 10(20145):272–286
25. Cai C, Chen J (2004) Direct electron transfer of glucose oxidase promoted by carbon nanotubes. Anal Biochem 332(1):75–83. https://doi.org/10.1016/j.ab.2004.05.057
26. Laviron E (1979) General expression of the linear potential sweep voltammogram in the case of diffusionless electrochemical systems. J Electroanal Chem Interfacial Electrochem 101(1):19–28. https://doi.org/10.1016/S0022-0728(79)80075-3

27. Shi Y, Li X, Ye M, Hu C, Shao H, Qu L (2015) An imperata cylindrical flowers-shaped porous graphene microelectrode for direct electrochemistry of glucose oxidase. J Electrochem Soc 162(7): B138–B144. https://doi.org/10.1149/2.0251507jes
28. Rabti A, Argoubi W, Raouafi N (2016) Enzymatic sensing of glucose in artificial saliva using a flat electrode consisting of a nanocomposite prepared from reduced graphene oxide, chitosan, nafion and glucose oxidase. Microchim Acta 183(3):1227–1233. https://doi.org/10.1007/s00604-016-1753-3
29. Xu J, Sheng Q, Shen Y, Zheng J (2017) Enhanced direct electron transfer of glucose oxidase based on gold nanoprism and its application in biosensing. Colloids Surf A Physicochem Eng Asp 529: 113–118. https://doi.org/10.1016/j.colsurfa.2017.05.049
30. Devasenathipathy R, Mani V, Chen S-M, Huang S-T, Huang T-T, Lin C-M, Hwa K-Y, Chen T-Y, Chen B-J (2015) Glucose biosensor based on glucose oxidase immobilized at gold nanoparticles decorated graphene-carbon nanotubes. Enzyme Microb Technol 78:40–45. https://doi.org/10.1016/j.enzmictec.2015.06.006
31. Hwa K-Y, Subramani B (2014) Synthesis of zinc oxide nanoparticles on graphene–carbon nanotube hybrid for glucose biosensor applications. Biosens Bioelectron 62:127–133. https://doi.org/10.1016/j.bios.2014.06.023
32. Kumar-Krishnan S, Hernandez-Rangel A, Pal U, Ceballos-Sanchez O, Flores-Ruiz FJ, Prokhorov E, Arias de Fuentes O, Esparza R, Meyyappan M (2016) Surface functionalized halloysite nanotubes decorated with silver nanoparticles for enzyme immobilization and biosensing. J Mater Chem B 4(15):2553–2560. https://doi.org/10.1039/C6TB00051G
33. Cao X, Ye Y, Li Y, Xu X, Yu J, Liu S (2013) Self-assembled glucose oxidase/graphene/gold ternary nanocomposites for direct electrochemistry and electrocatalysis. J Electroanal Chem 697:10–14. https://doi.org/10.1016/j.jelechem.2013.03.001